Localized amplification of energy in turbulent channels

By J. Jiménez†

1. Motivation

This paper is part of a wider inquiry into the relevance of linear dynamics to the large-scale structure of wall-bounded flows, in the spirit of del Álamo & Jiménez (2006). It has long been understood that some of the large-scale features of shear flows are governed by the linear behavior of the velocity perturbations, essentially because the production of turbulent energy from the mean shear is already present in the linearized equations. This is most easily seen in free shear flows, where the integral scales are well described by the unstable eigenfunctions of the mean velocity profile (Brown & Roshko 1974; Gaster *et al.* 1985), but Reynolds & Tiederman (1967) showed that the mean profiles of wall-bounded turbulent flows under moderate pressure gradients are stable, and it has been a matter of some discussion whether they nevertheless retain some traces of linear behavior. It was soon realized that the streamwise velocity streaks, which are the most obvious features of wall-bounded turbulent fields, originate from the essentially linear deformation of the mean profile by the wall-normal velocity, but quantitative agreement with experiments remained elusive.

In this paper we use x_j and u_j, with $j = 1 \dots 3$, for the streamwise, wall-normal and spanwise coordinates and velocity components, and bold-faced symbols represent vectors or matrices. The discussion is restricted to channels of half-width h, and the $^+$ superindex denotes wall units, defined from the friction velocity and the kinematic viscosity ν. Mean quantities are capitalized, and lower-case symbols are fluctuations.

The questions about the linearized dynamics in wall-bounded flows took a new turn when non-modal stability theory generalized rapid distortion theory to non-homogeneous cases, showing that stability does not necessarily mean lack of growth, and providing a wavenumber selection mechanism that was absent from previous analyses (Gustavsson 1991; Butler & Farrell 1992; Reddy & Henningson 1993; Schmid 2007). While that theory was originally developed for transition, it was eventually applied to turbulent velocity profiles, in the hope that the energy spectrum would be explained by which initial conditions are most strongly amplified. The initial results did not agree with observations. Even when Butler & Farrell (1993) analyzed the mean velocity profile of a turbulent channel, the most amplified perturbations had wavelengths $\lambda_3 = 2\pi/k_3 \approx 2h$, in the range of the large structures in the central part of turbulent channels, but the better-known sublayer streaks with $\lambda_3^+ \approx 100$ could not be recovered without artificial restrictions on the model.

A somewhat better agreement was obtained when del Álamo & Jiménez (2006) substituted the molecular viscosity in the equations by the eddy viscosity required to maintain the mean velocity profile. That model had previously been used in forced wall-bounded flows by Reynolds & Hussain (1972) and Jiménez *et al.* (2001), and the variation of eddy

† School of Aeronautics, Universidad Politécnica, 28040 Madrid, Spain

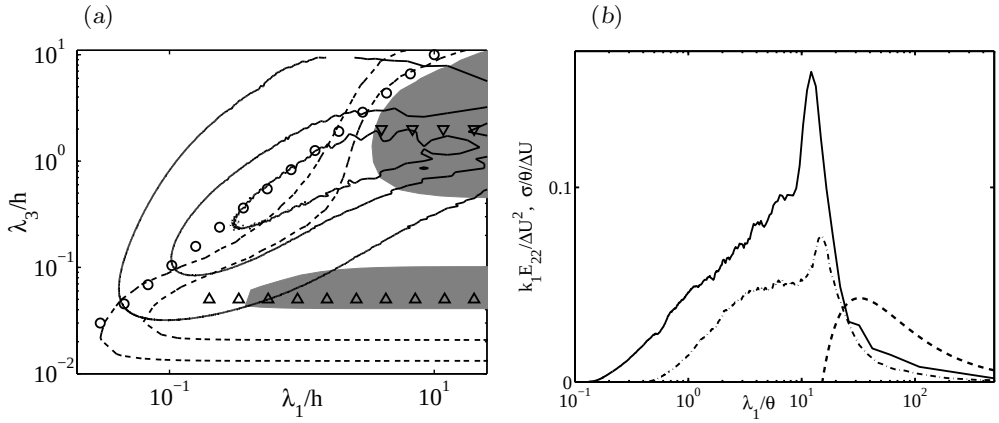

FIGURE 1. (a) The solid lines are the premultiplied spectrum (1.1) of the velocity magnitude, integrated over x_2, for the turbulent channel in Hoyas & Jiménez (2006) with $h^+ = 2003$. Contours are $(0.1, 0.4, 0.7)$ times the maximum of the spectrum. The dashed lines are the maximum energy amplification for initial conditions with a given wavevector (del Álamo & Jiménez 2006), using an eddy-viscosity fraction $\alpha = 0.6$ in (3.3). Contours are (2, 3, 4), and the highest contour is shaded. The symbols are: $\circ$, $\lambda_1 = \lambda_3$; $\triangle$, $\lambda_3^+ = 100$; $\triangledown$, $\lambda_3 = 2h$. (b) Premultiplied spectra of the cross-stream velocity component in a plane mixing layer, normalized with the local momentum thickness θ, and the velocity difference ΔU. —·— , $\Delta U\theta/\nu = 4000$; ——— , 12400. The dashed line is the normalized temporal growth rate for the instabilities of an error-function profile. Spectra from Delville *et al.* (1988).

viscosity with x_2 proved to be enough to produce two separate amplification peaks, with spanwise wavelengths corresponding to the outer structures and to the sublayer streaks. The shapes of the most amplified perturbations also agreed approximately with the leading proper-orthogonal modes of turbulent flows at those wavenumbers. That amplification map is compared in figure 1(a) to the integrated premultiplied energy spectrum for a turbulent channel,

$$k_1 k_3 \int_0^h E_{jj}(k_1,\, k_3, x_2)\, \mathrm{d}x_2, \tag{1.1}$$

where E_{jj} is the spectrum of u_j, and repeated symbols imply summation. This is the same energy norm used in the definition of the linear amplification.

While the agreement is suggestive, it is still imperfect, especially for the very elongated modes to the right of the figure. The amplification becomes independent of λ_1 for very long structures, while the spectrum decays beyond a given length. That is not obvious for the structures with $\lambda_3 \approx 2h$, where neither the available experiments nor the simulations extend much beyond those plotted in figure 1(a), but the sublayer streaks are known to have a definite length, of the order of $\lambda_1^+ \approx 10^4$ (Hoyas & Jiménez 2006). The agreement is even worse for the intermediate spanwise wavenumbers, corresponding to eigenfunctions peaking in the logarithmic layer. The amplification has a minimum in that range, but the spectral energy has a maximum.

In retrospect, there were few theoretical reasons to expect agreement, and it can be argued that at least three questions need to be addressed before deciding whether something should be expected from such comparisons. In the first place, even if we accept that linear growth is the primary mechanism for turbulent energy production, it is unclear why linear amplification, and especially the growth of a particular "optimum" initial

condition, should predict the nonlinear structures observed in the flow. While it is reasonable to assume that structures that are not amplified by the mean flow should not appear as energy-containing eddies in real turbulence, the converse is not obvious. Even in the better-understood case of free shear flows the correspondence is not straightforward, as shown in figure 1(b) for a plane turbulent shear layer. As in the wall-bounded case, the energy spectrum is not centered in the fastest growing wavelengths, but in the short-wavelength end of the unstable range. That was explained by Ho & Huerre (1984) as a consequence of the downstream thickening of the layer, which makes stability a function of x_1. As the structures move downstream, they drift towards shorter dimensionless wavelengths, until they eventually exit the unstable range. Unstable linear processes dominate because the time scale of the mean shear is faster than the nonlinearities, and the latter can only act once the instability disappears. For example, once the thickening of the layer removes a particular wavenumber from the linearly unstable regime, the eddies with those wavelengths either pair with their neighbors (Brown & Roshko 1974; Winant & Browand 1974) or are shredded by them (Moore & Saffman 1975), resulting in both cases in larger separations between the structures (Hernán & Jiménez 1982). The shorter wavelengths to the left of the stability boundary always decay nonlinearly into the standard energy cascade, which is probably the reason for the energy "leak" towards the left of the unstable ranges in figures 1(a) and 1(b). Note that this cascade is inhibited by viscosity for the very narrow wavelengths at the bottom of figure 1(b), which correspond to buffer-layer structures.

This explanation of the relative locations of the energy spectrum and the linearly amplified range is unlikely to apply to channels, which are equilibrium flows rather than evolving ones, forcing us to examine the rest of the approximations used in the linear analysis. The most obvious is the eddy viscosity model. The viscosity used by del Álamo & Jiménez (2006), $-\tau_{12}/\partial_2 U_1$, where τ_{12} is the total tangential stress, and $\partial_2 U_1 = \partial U_1/\partial x_2$, was probably too high to model correctly the energy-containing eddies. Those are also the eddies carrying most of the Reynolds stresses, and using the full viscosity neglects the stresses carried by them. In fact, the process of modeling the large scales using an eddy viscosity to represent the smaller ones is essentially large-eddy simulation, where it is known that the eddy viscosity should at least depend on the wavelength of the modes being neglected, and preferably also on the local state of the flow. On the other hand, although some "subgrid" model is required to provide turbulent dissipation, eddy viscosity is known to be only a crude approximation, and any result that depends too much on the details of the viscosity model should be treated with some caution.

This question, as well as the effects of nonlinearity and of the initial conditions, are beyond the scope of the present paper, and will be the subjects of future ones. Here we deal with a third problem that also separates turbulence from transition. The latter typically has a laminar base flow with a well-defined viscous lengthscale, and it makes sense for it to be studied in terms of global quantities, such as the amplification of the total kinetic energy. On the other hand, turbulence is a multiscale phenomenon, and different scales have to be treated more or less independently. For example, in modeling the energy spectrum in the logarithmic layer it is more useful to look at the amplification of the energy associated with those wall distances, rather than at the energy integrated over the whole flow. Another example is the modeling of individual velocity components. Unfortunately, energy measures that are restricted to a given geometrical neighborhood, or to a single velocity component, are rank-deficient in the sense that they vanish for some

non-zero flows, and as will be seen below, the standard formalism for optimal transient growth cannot be used for them.

The purpose of this paper is to introduce methods to compute optimally growing perturbations with respect to deficient norms, and to apply them to the modeling of the energy spectra at different wall distances in turbulent channels. The analytical scheme is presented in §2, and the application to the channel spectra is described in §3. The paper finally proposes some conclusions and future directions of research.

2. Optimum linear response of deficient norms

Consider the quadratic norm

$$\|\mathbf{u}\|_b^2 = \mathbf{u}^* B \mathbf{u} = \mathbf{u}^* b^* b \mathbf{u}, \tag{2.1}$$

where the asterisk stands for Hermitian conjugation. The matrix B is assumed Hermitian and positive semi-definite, so that it has a square root b. We reserve the symbol $\|\mathbf{u}\|^2 = \mathbf{u}^*\mathbf{u}$ for the Euclidean norm, so that $\|\mathbf{u}\|_b^2 = \|b\mathbf{u}\|^2$. Consider first the problem of maximizing the response of the forced linear system

$$(\partial_t - \mathrm{i}L)\mathbf{u} = D\mathbf{f}, \tag{2.2}$$

where i is the imaginary unit, and L and D are linear operators. We follow broadly the treatment in Schmid & Henningson (2001) and Schmid (2007), to which the reader is referred for details. Assume that $\mathbf{u}$ is expanded in terms of its Fourier components

$$\mathbf{u} = \widehat{\mathbf{u}}(x_2)\exp[\mathrm{i}(k_1x_1 + k_3x_3 - ck_1t)], \tag{2.3}$$

with a similar expansion for $\mathbf{f}$. The response of the system can be expressed as

$$\widehat{\mathbf{u}}(x_2) = \mathrm{i}\,(ck_1I + L)^{-1}D\widehat{\mathbf{f}}, \tag{2.4}$$

where I is the identity. The norm of $\widehat{\mathbf{u}}$ is then

$$\|\widehat{\mathbf{u}}\|_b^2 = \|b(ck_1I + L)^{-1}Db^{-1}b\widehat{\mathbf{f}}\|^2 \le \|b(ck_1I + L)^{-1}Db^{-1}\|\,\|\widehat{\mathbf{f}}\|_b^2, \tag{2.5}$$

and the maximum possible response $\|\widehat{\mathbf{u}}\|_b^2/\|\widehat{\mathbf{f}}\|_b^2$ is the maximum over the phase velocity c of the Euclidean matrix norm of M^*M, where

$$M = b(ck_1I - L)^{-1}Db^{-1}. \tag{2.6}$$

This is given by the largest singular value of M, and the optimum forcing is the corresponding singular vector. The difficulty is that, if B is deficient, the inverse b^{-1} does not exist.

The problem is not only formal. What we are trying to maximize is the response $\widehat{\mathbf{u}}$ to a unit forcing $\widehat{\mathbf{f}}$. Consider, for example, the maximum response of the u_1 velocity component to a perturbation of unit energy in that component. It is physically clear that it would almost surely be possible to find a forcing with no u_1 component, but whose response contains u_1. Such a forcing would result in an infinite amplification.

Jovanović & Bamieh (2005) solved this problem by requiring $\mathbf{u}$ and $\mathbf{f}$ to be in different subspaces, as in u_1 perturbations created by f_2 forces, with a complete norm for each quantity in its own subspace. However, that solution is slightly artificial, because it limits the search for the optimum forcing. Since in turbulence we are often interested in forcings that represent the effect of the neglected nonlinear terms, about which little is known, we will choose the alternative solution of using different norms for $\mathbf{f}$ and for $\mathbf{u}$. Only the

norm of $\mathbf{f}$ will be required to be complete. If we denote the target norm by $B = b^*b$, and the norm of $\mathbf{f}$ by $G = g^*g$, it follows from the derivation in (2.5) that the only modification required is to analyze the operator

$$M = b(ck_1 I + L)^{-1} D g^{-1}. \tag{2.7}$$

In particular, we will be interested in the case in which B is the kinetic energy integrated in the neighborhood of a given wall distance, while G is the kinetic energy integrated over the full channel.

The analysis of the initial-value problem follows similar lines. For example, assume that we want to study the evolution of $\mathbf{u}$ in

$$(\partial_t - \mathrm{i}L)\mathbf{u} = 0, \tag{2.8}$$

with initial conditions

$$\mathbf{u}(t=0) = \mathbf{u}_0. \tag{2.9}$$

Following again Schmid & Henningson (2001), the solution at time t is

$$\mathbf{u}(t) = \exp(\mathrm{i}Lt)\mathbf{u}_0, \tag{2.10}$$

and its norm can be written as

$$\|\mathbf{u}\|_b^2 = \|b\exp(\mathrm{i}Lt)\mathbf{u}_0\|^2 = \|b\exp(\mathrm{i}Lt)b^{-1}b\mathbf{u}_0\|^2. \tag{2.11}$$

If we wished to optimize the response $\|\mathbf{u}\|_b$ to a initial perturbation of unit norm $\|\mathbf{u}_0\|_b$, we would need to search for the maximum over time of the leading singular value of the matrix

$$M_1 = b\exp(\mathrm{i}Lt)b^{-1}. \tag{2.12}$$

The trailing b^{-1} has been introduced to allow the initial condition to be written as $b\mathbf{u}_0$, whose Euclidean norm we wish to be unity. As in the forced problem, this is not possible if B is deficient, and we need to solve the alternative problem of maximizing $\|\mathbf{u}\|_b$ for a unit initial norm $\|\mathbf{u}_0\|_g$, where g is nonsingular. It follows from arguments similar to those for forced systems that the only change required is to substitute (2.12) by

$$M_2 = b\exp(\mathrm{i}Lt)g^{-1}. \tag{2.13}$$

The analysis then proceeds as in Schmid & Henningson (2001), with the minor difference that it is no longer possible to substitute $b\exp(\mathrm{i}Lt)g^{-1}$ by the exponential of a constant matrix, $\exp(\mathrm{i}\,bLg^{-1}t)$.

3. The application to turbulent channels

We now apply this formalism to the spectral distribution of kinetic energy at a given distance from the wall in a turbulent channel. The equations of motion are those used by del Álamo & Jiménez (2006), with the later corrections by Pujals *et al.* (2009),

$$\left[(\partial_t + \mathrm{i}k_1U)\,\nabla^2 - \mathrm{i}k_1\partial_{22}U - \nabla^2\left(\nu_T\nabla^2\right) - 2k^2\partial_{22}\nu_T\right]\widehat{u}_2 = 0, \tag{3.1}$$

$$\left[\partial_t + \mathrm{i}k_1U - \partial_2\left(\nu_T\partial_2\right) + k^2\nu_T\right]\widehat{\omega}_2 + \mathrm{i}k_3\partial_2U\,\widehat{u}_2 = 0, \tag{3.2}$$

with boundary conditions $\widehat{u}_2 = \partial_2\widehat{u}_2 = \widehat{\omega}_2 = 0$ at the walls. The mean velocity profile is U, the wall-normal vorticity is ω_2, and $k^2 = k_1^2 + k_3^2$. The eddy viscosity is taken as a fraction α of the total eddy viscosity required to maintain the mean profile,

$$\nu_T/\nu = 1 + \alpha(\nu_C/\nu - 1), \tag{3.3}$$

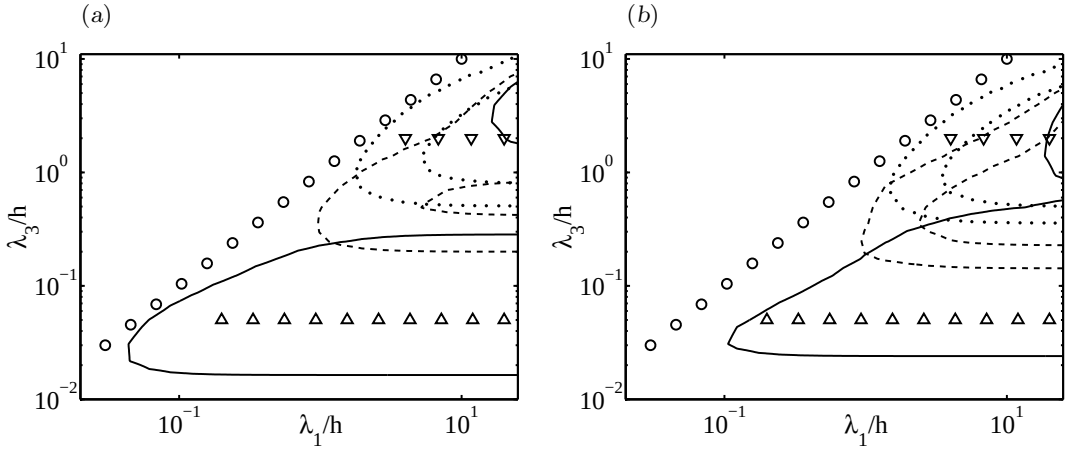

FIGURE 2. (a) Amplification of the local energy for a channel at $h^+ = 2000$. Gaussian energy window, as explained in the text. ——— , $(\delta \pm \sigma)/h = 0 \pm 0.015$; – – – –, 0.05 ± 0.01; ·····, 0.15 ± 0.03. Guide symbols as in figure 1. (a) Eddy-viscosity fraction $\alpha = 0.6$. The isolines are $A = 2.5$ and 7. (b) $\alpha = 0.2$. Isolines, $A = 6$ and 15.

where ν_C is taken to be the Cess (1958) approximation for the purpose of the calculation, as in del Álamo & Jiménez (2006). The mean velocity profile is the one corresponding to the full ν_C, so that the eddy viscosity does not carry the full Reynolds stress. The physical reason for this was sketched out in the introduction, although a more complete discussion will be deferred to a future article, but the main reason to introduce here the factor α is to verify that the results are not overly dependent on the details of ν_T. We shall see that the effect of α is mainly to change the amplification factors, without changing the wavenumbers involved. Most of the present calculations use $\alpha = 0.6$, which was found by Flores & Jiménez (2009) to reproduce approximately the decay rate of the u_2 perturbations in a particular linearized model of the channel.

We are interested in the perturbations that are most strongly amplified in the neighborhood of a given wall distance, starting from perturbations with unit energy defined over the full channel. In particular, we will define the full norm $\|\widehat{\mathbf{u}}\|_g^2$ as the integral of $\|\widehat{\mathbf{u}}\|^2(x_2)$ over the whole channel, and the deficient one as the weighted integral

$$\|\widehat{\mathbf{u}}\|_b^2 = \int_0^h \|\widehat{\mathbf{u}}\|^2(x_2)\, W(x_2)\, \mathrm{d}x_2, \tag{3.4}$$

where the weight W is a Gaussian window of the form $\exp[-(x_2-\delta)^2/2\sigma^2]$, symmetrized with respect to the channel centerline and to each wall. If σ is chosen small enough, $\|\widehat{\mathbf{u}}\|_b^2$ isolates the energy of each Fourier mode in the neighborhood of δ, and therefore the spectrum at that height.

Although the problem of maximizing $\|\widehat{\mathbf{u}}\|_b(t)$ for a given initial $\|\widehat{\mathbf{u}}\|_g(0)$ is well posed, the ratio of the two quantities is not relevant, because the two norms measure different properties. After computing the optimum initial condition, and the maximum growth of $\|\widehat{\mathbf{u}}\|_b(t)/\|\widehat{\mathbf{u}}\|_g(0)$, we therefore define the amplification as

$$A(t;\delta,\sigma) = \|\widehat{\mathbf{u}}\|_b^2(t)/\|\widehat{\mathbf{u}}\|_b^2(0). \tag{3.5}$$

Some representative results are shown in figure 2(a), which contains three narrow energy windows at different distances to the wall. As could intuitively be expected, the

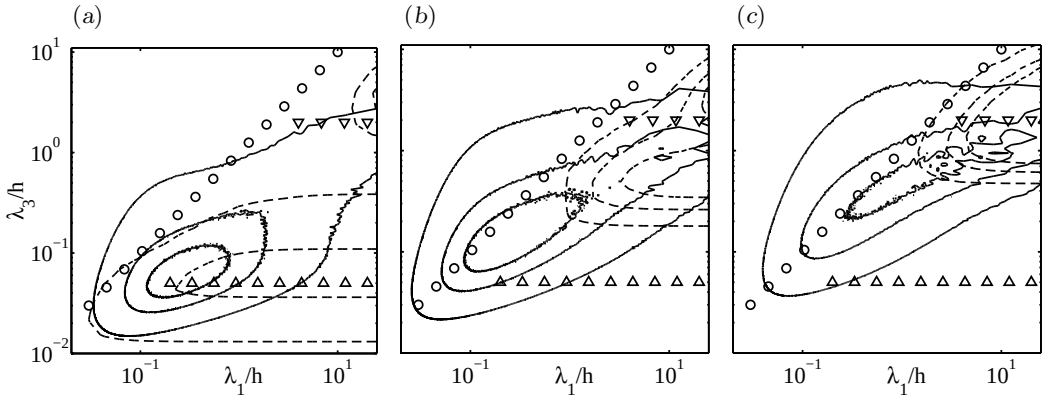

FIGURE 3. Amplification of the local energy for a channel at $h^+ = 2000$, $\alpha = 0.6$, using Gaussian energy windows, compared to premultiplied total-energy spectra from Hoyas & Jiménez (2006), weighted with the same windows. - - - -, Energy amplification. Isolines are $A = 2$, 4, 6; ——, weighted spectra. Isolines are (0.1, 0.4, 0.7) times the maximum of each spectrum. Guide symbols as in figure 1. (*a*) $(\delta \pm \sigma)/h = 0 \pm 0.015$; (*b*) 0.05 ± 0.01; (*c*) 0.15 ± 0.03.

perturbations that are most amplified over the window spanning the buffer layer recover spanwise wavelengths of the order of the sublayer streaks ($\lambda_3^+ \approx 100$), while the window spanning mostly outer layers, $x_2 = 0.15 \pm 0.03$, recovers only outer wavelengths ($\lambda_3 \approx 2h$). There is relatively little change for windows higher than this one. Within the limited range of intermediate scales available for the Reynolds number in figure 2, an energy window intermediate between the previous two recovers intermediate spanwise wavelengths, in agreement with the vertical structure of the spectra, and of the leading proper orthogonal modes in that range of wavenumbers (del Álamo & Jiménez 2006; Hoyas & Jiménez 2006).

Note that the large-scale modes ($\lambda_3 \approx 2h$) appear in the amplification maps of all the energy windows, including those restricted to the buffer layer, emphasizing that those "global" modes contribute energy to all wall distances (del Álamo & Jiménez 2003; Hoyas & Jiménez 2006). It is also interesting that the amplification factors for the "logarithmic" intermediate window are comparable to those of the other two, even if they lie in the region of minimum amplifications for the total energy in figure 1(*a*).

To test the robustness of the results, figure 2(*b*) repeats figure 2(*a*) with a lower fraction of the eddy viscosity ($\alpha = 0.2$). Both figures are very similar, except that the amplifications are somewhat higher in the lower-viscosity case. This is in contrast to the results of Butler & Farrell (1993), who could only recover the sublayer streaks by imposing artificial restrictions on the time scales allowed for the growth. On the other hand, some amount of variable viscosity seems to be important to differentiate between the buffer layer and the outer flow. If the same problem is run with a constant molecular viscosity at the same Reynolds number ($\alpha = 0$), the energy window peaking at the wall still isolates wavelengths which are narrower than those of the total energy, but those "buffer layer" structures become wider ($\lambda_3^+ \approx 400$). Nevertheless, it is interesting that the amplifications of the narrower norms are considerably less sensitive to the details of the eddy viscosity than those based on the full one, probably because part of the wavelength selection role of the variable viscosity is taken over by the weighting window. For example, when using the full norm in the channel, the minimum eddy viscosity that still gives two amplification maxima is of the order of $\alpha = 0.5$.

The amplification factors of the local energy are compared in figure 3 to the correspond-

ing weighted spectra, giving some extra information on the reasons for the discrepancy of the two quantities. It appeared from figure 1(*a*) that the spectrum of the total energy was located in the short-λ_1 edge of the amplified region, but it is seen here that it actually lies in the small-wavelength edge of both λ_1 and λ_3. This happens roughly along the isotropic direction $\lambda_3 = \lambda_1$, suggesting some kind of nonlinear cascade, probably both in wavenumber and along x_2. That suggestion is reinforced by the better agreement between the spectrum and the amplified region in the buffer layer, where the cascade is blocked by viscosity. However, the results are sensitive to the details of the weighting window, both for the amplification and for the weighted spectra, and the disagreement in figure 3 may be partly due to an "inadequate" window choice, which was chosen here mostly to demonstrate the method. Physically relevant results would require considering at least some of the other factors discussed in the introduction. A somewhat better agreement is found for the $-\langle u_1 u_2 \rangle$ cospectra, which may be a more relevant quantity than $\|\mathbf{u}\|^2$, because the amplification is intended to model the energy production, but the agreement is not good enough to consider the problem as solved.

Linear effects cannot change the wavenumbers, and any nonlinear cascade is outside the linearized models discussed here, but it may be possible to learn something about the energy redistribution along x_2 by the temporal evolution of the initial perturbations. The general character of the most amplified perturbations isolated by the present analysis is similar, although not identical, to that of the optimal perturbations obtained from the amplification of the total energy (for example, see figure 5 in del Álamo & Jiménez 2006). In both cases, an array of weak quasi-streamwise vortices gives rise to much stronger streaks of the streamwise velocity. The initial vortices typically decay monotonically, but in the process they move, or diffuse, farther away from the wall by factors of the order of 1.5 or 2. The streaks are always created closer to the wall than the original vortices, because the growth is strongest where the shear is steepest. This is the classical mechanism for streak generation, discussed, for example, by Bakewell & Lumley (1967) or Kim *et al.* (1971).

There is an interesting group of modes, with moderate amplifications of $O(2-3)$, in which the growth happens directly in the transverse velocity components $(u_2 - u_3)$. They are the roughly isotropic structures in the "nose" of the wide-wavelength peaks in figures 1(*a*) and 3(*c*), and they are vortices that are initially tilted backwards and get rotated forward by the shear. The maximum amplification occurs at the moment in which they are roughly vertical. A very similar behavior is found for the inviscid rapid-distortion of vortices in a uniform shear (Orr 1907), where it is associated with the relaxation of the vertical continuity constraint as the structures rotate and $\partial_2 u_2 \to 0$. This behavior is observed both for cases based on the amplification of total energy, and for those based on windows for which those modes contribute to the local energy.

In general, the main difference between the present structures and those obtained from the full energy is that they are narrower in x_2, peaking more steeply near the center of the weighting window. The envelope of the spectral regions in which the *total* energy is amplified for windows of different heights agrees well with the overall amplification region given in figure 1(*a*), so that all the perturbations that are locally amplified are also amplified globally, but higher amplification isolines differ significantly between the two problems.

4. Conclusions and future work

We have presented a simple modification of the classical analysis of optimum non-modal amplification in linear evolution equations that permits the optimization of the growth of incomplete seminorms, such as the energy associated with a given distance to the wall in a turbulent channel. The norm used to normalize the initial condition, or the forcing in forced systems, still must be complete.

We have applied the scheme to modeling the energy spectra in turbulent channels at different distances from the wall, using a weighting window to isolate the energy growth at those distances. As the window is moved away from the wall, the most amplified perturbations isolate the spanwise wavelengths characteristic of the spectra at those locations, although as in the case of the analysis of the full energy, the correspondence is only imperfect. As in the latter case, the growth mechanism is typically the formation of streamwise-velocity streaks from an initial array of quasi-streamwise vortices, but the amplification of the roughly isotropic global modes, with wavelengths of the order of the channel width, can be traced to the essentially inviscid mechanics of the transverse velocity. By varying the eddy viscosity, we have shown that the amplification dynamics are only weakly dependent on the details of the viscosity model, although some eddy viscosity is required to differentiate between the buffer layer and the outer flow.

Several avenues for future investigations were proposed in the introduction, and other have been suggested throughout the subsequent discussion. Some obvious generalizations concern more inhomogeneous flows, such as boundary layers with adverse pressure gradients (Corbett & Bottaro 2000), in which the location of the peak energy production is known to change, but perhaps the most immediate task is the resolution of the discrepancy between the linearly amplified region and the observed spectra. Although the present analysis makes the disagreement more specific, by relating the wall distance to the spanwise wavelength, it still does not explain why the amplification does not decay for very long streamwise wavelengths, whereas the spectra do. Several possibilities have already been mentioned, but the most promising is the introduction of a spectral dependence in the eddy viscosity, for which we have given physical reasons. Even if we have argued above that the details of that dependence should not be too critical for the final result, it makes physical sense that the longer wavelengths, which have longer "subgrid" ranges, should feel a higher eddy viscosity, which would result in lower amplifications. Preliminary results of García-Ramos & Jiménez (2009) suggest that this is indeed the case.

Acknowledgments

This work was supported in part by the CICYT grant TRA2006-08226, and by the Advanced Simulation and Computing program of the Department of Energy. The exceptionally careful criticism by J. W. Nichols of a preliminary version of this manuscript is gratefully acknowledged.

REFERENCES

del Álamo, J. C. & Jiménez, J. 2003 Spectra of the very large anisotropic scales in turbulent channels. *Phys. Fluids* **15**, L41–L44.

del Álamo, J. C. & Jiménez, J. 2006 Linear energy amplification in turbulent channels. *J. Fluid Mech.* **559**, 205–213.

Bakewell, H. P. & Lumley, J. L. 1967 Viscous sublayer and adjacent wall region in turbulent pipe flow. *Phys. Fluids* **10**, 1880–1889.

Brown, G. L. & Roshko, A. 1974 On the density effects and large structure in turbulent mixing layers. *J. Fluid Mech.* **64**, 775–816.

Butler, K. M. & Farrell, B. F. 1992 Three-dimensional optimal perturbations in viscous shear flow. *Phys. Fluids A* **4**, 1637–1650.

Butler, K. M. & Farrell, B. F. 1993 Optimal perturbations and streak spacing in wall-bounded shear flow. *Phys. Fluids A* **5**, 774–777.

Cess, R. D. 1958 A survey of the literature on heat transfer in turbulent tube flow. Report 8-0529-R24. Westinghouse Research.

Corbett, P. & Bottaro, A. 2000 Optimal perturbations of boundary layers subject to stream-wise pressure gradient. *Phys. Fluids* **12**, 120–130.

Delville, J., Bellin, J. H. & Bonnet, J. P. 1988 Analysis of structures in a turbulent mixing layer using a pseudo-flow visualization method based on hot-wire anemometry. In *Advances in turbulence II* (ed. H. H. Fernholz & H. Fiedler), pp. 251–256. Springer, case SHL04 in AGARD Advisory Rep. 345.

Flores, O. & Jiménez, J. 2009 Log-layer dynamics in smooth and artificially-rough turbulent channels. In *IUTAM symp. on flow over rough walls* (ed. T. B. Nickels). Springer.

García-Ramos, P. & Jiménez, J. 2009 Initial conditions and symmetry breaking for linear energy amplification in eddy-viscosity models of turbulent channels. In *Proc. Div. Fluid Dyn.*, pp. LA–03. Am. Phys. Soc.

Gaster, M., Kit, E. & Wygnanski, I. 1985 Large-scale structures in a forced turbulent mixing layer. *J. Fluid Mech.* **150**, 23–39.

Gustavsson, L. H. 1991 Energy growth of three-dimensional disturbances in plane Poiseuille flow. *J. Fluid Mech.* **224**, 241–260.

Hernán, M. A. & Jiménez, J. 1982 Computer analysis of a high-speed film of the plane turbulent mixing layer. *J. Fluid Mech.* **119**, 323–345.

Ho, C. H. & Huerre, P. 1984 Perturbed free shear layers. *Ann. Rev. Fluid Mech.* **16**, 365–424.

Hoyas, S. & Jiménez, J. 2006 Scaling of the velocity fluctuations in turbulent channels up to $Re_\tau = 2003$. *Phys. Fluids* **18**, 011702.

Jiménez, J., Uhlmann, M., Pinelli, A. & Kawahara, G. 2001 Turbulent shear flow over active and passive porous surfaces. *J. Fluid Mech.* **442**, 89 – 117.

Jovanović, M. R. & Bamieh, B. 2005 Componentwise energy amplification in channel flows. *J. Fluid Mech.* **534**, 145–183.

Kim, H. T., Kline, S. J. & Reynolds, W. C. 1971 The production of turbulence near a smooth wall in a turbulent boundary layer. *J. Fluid Mech.* **50**, 133–160.

Moore, D. W. & Saffman, P. G. 1975 The density of orgamized vortices in a turbulent mixing layer. *J. Fluid Mech.* **69**, 465–473.

Orr, W. M. 1907 Stability or instability of the steady motions of a perfect liquid and of a viscous liquid. *Proc. Roy. Irish Acad.* **A 27**, 9–138.

Pujals, G., García-Villalba, M., Cossu, C. & Depardon, S. 2009 A note on optimal transient growth in turbulent channel flow. *Phys. Fluids.* **21**, 015109.

Reddy, S. C. & Henningson, D. S. 1993 Energy growth in viscous channel flows. *J. Fluid Mech.* **525**, 209 – 238.

Reynolds, W. C. & Hussain, A. K. M. F. 1972 The mechanics of an organized wave in

turbulent shear flow. Part 3. Theoretical models and comparisons with experiments. *J. Fluid Mech.* **54**, 263–288.

Reynolds, W. C. & Tiederman, W. G. 1967 Stability of turbulent channel flow, with application to Malkus' theory. *J. Fluid Mech.* **27**, 253–272.

Schmid, P. J. 2007 Nonmodal stability theory. *Ann. Rev. Fluid Mech.* **39**, 129–162.

Schmid, P. J. & Henningson, D. S. 2001 *Stability and transition in shear flows*. Springer.

Winant, C. D. & Browand, F. K. 1974 Vortex pairing: the mechanism of turbulent mixing-layer growth at moderate Reynolds number. *J. Fluid Mech.* **63**, 237–255.